Stress Analysis of a Mode I Edge Delamination Specimen for Composite Materials

James M. Whitney*
Air Force Wright Aeronautical Laboratories, Wright-Patterson Air Force Base, Ohio

A higher-order laminated plate theory which includes transverse shear deformation and a thickness-stretch mode is utilized to analyze a mode I edge delamination specimen, including thermal residual stresses. The analysis allows one to obtain an approximate distribution of the interlaminar normal stress ahead of the crack and to investigate the effect of specimen geometry on strain energy release rate. Both tension and compression loading are considered. Numerical results indicate that thermal residual stresses can have a significant effect on both the stress distribution ahead of the crack and the mode I strain energy release rate.

Introduction

IT has been recognized that for certain stacking geometries delamination can be produced along the free edges of a simple laboratory laminated composite tensile coupon. Pagano and Pipes[1] proposed such a test to characterize the interlaminar tensile (peel) strength of laminated composite materials. O'Brien[2] has extended this concept to the study of delamination onset and growth in graphite/epoxy laminates. He utilized a $[\pm 30_2/90/90]_s$ laminate subjected to uniaxial tensile loading. A strain energy release rate calculation was also developed in conjunction with this free-edge delamination coupon.

Difficulties arise, however, in conjunction with the edge delamination test (EDT). In particular, the crack growth from the edges is neither uniform nor symmetric. The edge crack does not remain in the laminate midplane, but oscillates between the midplane and the $90/-30$ interfaces, producing a mixed-mode fracture rather than a pure mode I delamination.

Recently, an edge delamination specimen has been developed which will produce mode I behavior.[3] As illustrated in Fig. 1, this specimen consists of a straight-sided tensile coupon with starter cracks in the form of embedded strips of homogeneous material. These strips are placed along the free edges at the laminate midplane for the purpose of inducing a mode I delamination response. The specimen width is denoted by $2b$ and the crack length by a. Tensile loading is applied to the specimen until the crack begins to propagate toward the center of the coupon. At the onset of crack propagation, there is an abrupt change in the stress-strain curve, as illustrated in Fig. 1. The strain level at which the crack moves is denoted by ϵ_c. This critical strain level can then be used in conjunction with the equation shown in Fig. 1 to calculate the mode I critical strain energy release rate G_{Ic}. This relationship is based on classical laminated plate theory (CPT) in the absence of residual stresses induced by temperature and moisture. In this relationship E_x denotes the modulus of a specimen without an edge delamination, while E^* denotes the modulus of each delaminated half after the crack has propagated completely across the width of the specimen.

Received Jan. 30, 1985; presented as Paper 85-0611 at the AIAA/ASME/ASCE/AHS Structures, Structural Dynamics and Materials Conference, Orlando, FL, April 15-17, 1985, revision received Nov. 6, 1985.

*Materials Research Engineer, Nonmetallic Materials Division of the Materials Laboratory; also Adjunct Professor, University of Dayton, Ohio. Associate Fellow AIAA.

In Ref. 3 an energy release rate expression which included the effect of residual stresses was derived in conjunction with the specimen illustrated in Fig. 1. This analysis was also based on CPT. Such an approach, however, precludes any estimation of the interlaminar normal stress distribution ahead of the crack and resulting transient effects of specimen geometry on mode I strain energy release rate.

In the present paper a higher-order plate theory is used in conjunction with a procedure suggested by Pagano,[4] in order to determine an approximation to the interlaminar normal stress distribution ahead of the crack and the resulting transient influence of specimen geometry on mode I strain energy release rate. Such an approach has been successfully applied to a double cantilever beam specimen.[5] Numerical results are obtained for 12-ply laminates of the class $[\theta/-\theta_2/\theta/90_2]_s$ and for the class $[0_3/90_3]_s$.

Analysis

Because of symmetry considerations only the upper right quarter of the plate, as illustrated in Fig. 2, need be considered. Symmetry also dictates that the transverse displacement w and the interlaminar shear stresses τ_{xz} and τ_{yz} must vanish at the laminate midplane in the uncracked region. Thus in this region the normal surface traction at $z=-h/2$ is treated as a dependent variable. In the cracked region the surface at $z=-h/2$ is free, and all tractions must vanish. The analysis assumes cylindrical bending, i.e., all force and moment resultants are independent of x.

As previously discussed by Pagano,[4] there are certain minimum requirements that must be met by the plate theory chosen to attack the problem shown in Fig. 2. In particular, if we choose CPT to solve the problem, we find that the normal stress on the surface $z=-h/2$ vanishes identically. This difficulty can be overcome by considering a laminated plate theory which includes the effects of transverse shear deformation.[6] In this case, however, the transverse displacement w is independent of z, and by prescribing $w=0$ at the surface $z=-h/2$ we force w to vanish throughout the uncracked region of the plate. Such a constraint does not allow the transverse shear force resultant Q_y to be prescribed at both ends ($y=0$, $y=-b$), leading to either a discontinuity in Q_y at $y=0$ or an incorrect value of Q_y at $y=-b$ Thus, as concluded by Pagano,[4] the simplest appropriate theory must include both transverse shear deformation and thickness-stretch deformation mode. A modified form of the Whitney-Sun laminated plate theory,[7] as utilized by Pagano[4] for free-edge stress analysis, meets the minimum requirements and will be applied to the problem shown in Fig. 2. The analysis

is based on the following displacement field:

$$u = x\epsilon + u^0(y) + z\Omega(y) \tag{1}$$

$$v = v^0(y) + z\psi(y) \tag{2}$$

$$w = w^0(y) + z\phi(y) \tag{3}$$

where u, v, and w denote displacements relative to the x, y, and z axes, respectively, and ϵ is a uniform axial strain.

Thus, the analysis is based on modified plane strain conditions. Replacing the subscripts x, y, z, yz, xz, and xy by the subscripts 1-6, respectively, the constitutive relations can be written in the form

$$N_i = A_{ij}\epsilon_j^0 + B_{ik}\kappa_k - N_i^T \qquad (i,j = 1,2,3,6;\ k = 1,2,6) \tag{4}$$

$$M_i = B_{ij}\epsilon_j^0 + D_{ik}\kappa_k - M_i^T \qquad (j = 1,2,3,6;\ i,k = 1,2,6) \tag{5}$$

$$N_i = k(A_{ij}\epsilon_j^0 + B_{ij}\kappa_j) \qquad (i,j = 4,5) \tag{6}$$

$$M_i = k(B_{ij}\epsilon_j^0 + D_{ij}\kappa_j) \qquad (i,j = 4,5) \tag{7}$$

where, denoting partial differentiation by a comma, we have

$$\epsilon_1^0 = \epsilon, \quad \epsilon_2^0 = v^0_{,y}, \quad \epsilon_3^0 = \phi, \quad \epsilon_4^0 = \psi + w^0_{,y}, \quad \epsilon_5^0 = \Omega, \quad \epsilon_6^0 = u^0_{,y} \tag{8}$$

$$\kappa_1 = 0, \quad \kappa_2 = \psi_{,y}, \quad \kappa_4 = \phi_{,y}, \quad \kappa_5 = 0, \quad \kappa_6 = \Omega_{,y} \tag{9}$$

In addition, the following definitions are used:

$$(A_{ij}, B_{ij}, D_{ij}) = \int_{-h/2}^{h/2} C_{ij}(1, z, z^2)\,dx \tag{10}$$

where C_{ij} is a ply stiffness coefficient, and

$$(N_i, M_i) = \int_{-h/2}^{h/2} \sigma_i(1, z)\,dz \tag{11}$$

In Eq. (11), σ_i denotes ply stress components. The terms with the superscript T denote thermal force and moment resultants which are included for the purpose of determining the effect of residual stresses due to laminate fabrication on the EDT specimen. These terms are defined as follows:

$$(N_i^T, M_i^T) = \Delta T \int_{-h/2}^{h/2} Q_{ij}\alpha_j(1, z)\,dz \qquad (i,j = 1,2,6) \tag{12}$$

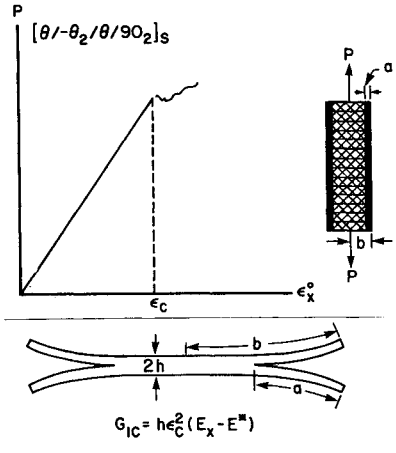

Fig. 1 Edge delamination test.

$$N_3 = \Delta T \int_{-h/2}^{h/2} C_{3j}\alpha_j\,dz \qquad (j = 1,2,3,6) \tag{13}$$

where Q_{ij} and α_j are the ply reduced stiffness for plane stress and the ply thermal coefficient of linear expansion, respectively. In Eqs. (4-7), (12), and (13), summation is implied by repeated indices. The use of the reduced stiffnesses Q_{ij} in Eq. (12) rather than C_{ij} will be discussed later. The temperature differential ΔT is the difference between use temperature—room temperature for the present purposes—and the stress-free temperature, which is usually below the laminate cure temperature. A shear correction factor k is introduced into Eqs. (6) and (7) in order to improve the accuracy of the theory. For the present paper the value $k = 5/6$ derived by Medwadowski[8] for homogeneous, orthotropic materials is utilized.

The equilibrium equations take the form[4]

$$N_{xy,y} = 0 \tag{14a}$$

$$N_{y,y} = 0 \tag{14b}$$

$$N_{yz,y} - q = 0 \tag{14c}$$

$$M_{y,y} - N_{yz} = 0 \tag{14d}$$

$$M_{yz,y} = N_z + qh/2 = 0 \tag{14e}$$

$$M_{xy,y} - N_{xz} = 0 \tag{14f}$$

where

$$q = \sigma_z(y, -h/2) \tag{15}$$

Equations (14a) and (14b) in conjunction with the free-edge boundary conditions at $y = a$ imply that

$$N_y = N_{xy} = 0 \tag{16}$$

Substitution of the constitutive relations, Eqs. (4-9), into Eqs. (14a-14f) leads to six equations in the six kinematic variables of Eqs. (1-3). In addition, for the class of laminates $[\theta/-\theta_2/\theta/90_2]_T$ we find

$$A_{16} = A_{26} = A_{36} = A_{45} = B_{16} = B_{26} = B_{36} = B_{45} = 0$$

$$N_{xy}^T = M_{xy}^T = 0 \tag{17}$$

For the cylindrical bending assumptions displayed in Eqs. (1-3), however, D_{16} never appears in the governing equations. Thus D_{26} is the only shear coupling coefficient that one must deal with for this class of laminates. In addition, D_{26} is an order of magnitude smaller than the other in-plane bending coefficients D_{22} and D_{66} which appear in the governing equations. Thus the shear coupling is extremely weak for this class of laminates. As a result, the D_{26} coupling is neglected in the present paper, which leads to the simplification

$$u^0(y) = \Omega(y) = 0 \tag{18}$$

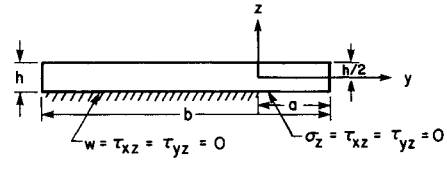

Fig. 2 Nomenclature for the stress analysis model.

All of the equilibrium equations, with the exception of Eq. (14f), can be satisfied exactly by Eq. (18). For the class of laminates $[0_3/90_3]_T$, $D_{16}=D_{26}=0$, and Eq. (18) is an exact solution to the governing equations.

As illustrated in Fig. 2, two intervals along the y axis are considered. In the interval $-(b-a)\le y\le 0$, symmetry dictates that $w(y,-h/2)=0$, and Eq. (3) yields

$$w^0=\tfrac{1}{2}h\phi \tag{19}$$

The surface traction q now becomes a dependent variable. In the interval $0\le y\le a$, $q=0$, and the four kinematic variables in Eqs. (2) and (3) become the dependent variables.

Equations (14c) and (14d), along with the free-edge boundary conditions at $y=a$, lead to result

$$N_{yz}=M_y=0 \qquad (0\le y\le a) \tag{20}$$

The solution to the governing equations will consist of a particular solution and a homogeneous solution. For laminates in which $b-a>2h$, the exact solution outside of the boundary zone $-(b-a)\le y\le -2h$ is provided by CPT, in which each ply is assumed to be in a state of plane stress.[9] Thus, in order to improve the accuracy of the results, the particular solutions are developed in terms of CPT stiffnesses and thermal terms, with the stiffness coefficients as defined in Eq. (10) being replaced by

$$(A'_{ij},B'_{ij},D'_{ij})=\int_{-h/2}^{h/2} Q_{ij}(1,z,z^2) \qquad (i,j=1,2) \tag{21}$$

The thermal terms are given by Eq. (12). For consistency, Eqs. (12) and (21) are used in conjunction with the particular solutions in both regions of the plate under consideration.

Stress Distribution Ahead of the Crack

We now consider the solution in the region $-(b-a)\le y\le 0$. Continuity conditions at $y=0$ in conjunction with Eq. (20) lead to the requirement

$$N_{yz}(0)=M_y(0)=0 \tag{22}$$

Along the centerline of the plate we require

$$\psi(a-b)=N_{yz}(a-b)=0 \tag{23}$$

Equations (18-20), (22), and (23) form the basis of an identical problem solved by Pagano.[4] For laminates in which $b-a>2h$, the stress distribution ahead of the crack may be written in the form[4]

$$q=\frac{\lambda_1\lambda_2}{\lambda_1-\lambda_2}(\lambda_1 e^{\lambda_1\bar{y}}-\lambda_2 e^{\lambda_2\bar{y}})M_0 \tag{24}$$

where $\bar{y}=y/h$ and

$$M_0=[A'_{22}B'_{12}-A'_{12}B'_{22})\epsilon+B'_{22}N_y^T-A'_{22}M_y^T]/A'_{22} \tag{25}$$

Values of λ_i are determined from the roots of a characteristic equation, which leads to the result

$$\lambda_{1,2}=\sqrt{-r_2\pm\sqrt{r_2^2-4r_1r_3}/2r_1} \tag{26}$$

where r_i is expressed in terms of the stiffnesses A_{ij}, B_{ij}, and D_{ij} as defined by Pagano.[4] For the materials considered in the present paper, λ_i is real, so that Eq. (24) is valid.

Mode I Strain Energy Release Rate

The mode I strain energy release rate can be determined by considering the work done by the external forces,[3] with the result

$$G_I=-\frac{dw}{da} \tag{27}$$

where

$$W=\int_{-(b-a)}^{0}(\epsilon-\epsilon_1^T)N_{x1}\,dy+\int_0^a(\epsilon-\epsilon_2^T)N_{x2}\,dy \tag{28}$$

In Eq. (28) the subscripts 1 and 2 refer to values in the regions $-(b-a)\le y\le 0$ and $0\le y\le a$, respectively. The quantity ϵ_i^T is the effective free thermal expansion strain for the ith region as derived from CPT and is given by the relations

$$\epsilon_1^T=\frac{A'_{22}N_x^T-A'_{12}N_y^T}{A'_{11}A'_{22}-A'^2_{12}}$$

$$\epsilon_2^T=\frac{\bar{A}_1N_x^T-\bar{A}_2N_y^T-\bar{A}_3M_y^T}{A'_{11}\bar{A}_1-A'_{12}\bar{A}_2+B'_{12}\bar{A}_3}$$

where

$$\bar{A}_1=A'_{22}D'_{22}-B'^2_{22}$$

$$\bar{A}_2=A'_{12}D'_{22}-B'_{12}B'_{22}$$

$$\bar{A}_3=A'_{22}B'_{12}-A'_{12}B'_{22}$$

From Pagano's solution[4] N_{x1} can be written in the form

$$N_{x1}=E_xh(\epsilon-\epsilon_1^T)+\sum_{i=1}^{2}A_ie^{\lambda_i\bar{y}} \tag{29}$$

where A_i is a function of λ_i, A_{ij}, B_{ij}, and D_{ij}. As previously mentioned, E_x is the effective modulus in the x direction as determined from CPT for the laminate in the absence of free-edge delamination ($a=0$), with the result

$$E_x(A'_{11}A'_{22}-A'^2_{12})/hA'_{22}$$

To obtain N_{x2} we consider the solution to the governing equations applicable to the region $0\le y\le a$. Applying the condition $N_y=0$, we find

$$v^0_{h,y}=(-B_{22}\psi_{h,y}-A_{23}\phi_h)/A_{22} \tag{30}$$

$$v^0_{p,y}=(-A'_{12}\epsilon-B'_{22}\psi_{p,y}+N_y^T)/A'_{22} \tag{31}$$

where the subscripts h and p refer to homogeneous and particular solutions, respectively. Similarly, applying the condition $N_{yz}=0$, we find

$$w^0_{h,y}=-\psi_h-(B_{44}/A_{44})\phi_{h,y} \tag{32}$$

$$w^0_{p,y}=-\psi_p \tag{33}$$

Substituting Eqs. (4-9) into Eq. (14e) and taking into account Eqs. (30-33) along with the relationship $M_y=0$, we obtain the homogeneous equations

$$D_1\psi_{h,y}+D_2\phi_h=0 \tag{34}$$

$$D_2\psi_{h,y}-(A_{22}/A_{44})D_3\phi_{h,yy}+D_4\phi=0 \tag{35}$$

where

$$D_1=A_{22}D_{22}-B_{22}^2$$

$$D_2=A_{22}B_{23}-A_{23}B_{22}$$

$$D_3=k(A_{44}D_{44}-B_{44}^2)$$

$$D_4=A_{22}A_{33}-A_{23}^2$$

along with the particular solutions

$$v_p^0 = -y\,\frac{(A'_{12}D_{22} - B'_{22}B'_{12})\epsilon - D'_{22}N_y^T + B'_{22}M_y^T}{A'_{22}D'_{22} - (B'_{22})^2} \tag{36}$$

$$\psi_p = -y\,\frac{(A'_{22}B'_{12} - A'_{12}B'_{22})\epsilon + B'_{22}N_y^T - A'_{22}M_y^T}{A'_{22}D'_{22} - (B'_{22})^2} \tag{37}$$

The axial force resultant can be written in the form

$$N_{x2} = E^*h(\epsilon - \epsilon_2^T) + \frac{A_{22}A_{13} - A_{12}A_{23}}{A_{22}}\,\phi_h + \frac{A_{22}B_{12} - A_{12}B_{22}}{A_{22}}\,\psi_{h,y} \tag{38}$$

where E^* is the effective modulus in the x direction, as determined from the particular solutions, for a laminate in which the delamination extends completely across the width of the laminate ($a = b$) and is given by the relationship[3]

$$E^* = (A'_{11}\bar{A}_1 - A'_{12}\bar{A}_2 + B'_{12}\bar{A}_3)/\bar{A}_1 h$$

Solving Eqs. (34) and (35), we find

$$\psi_h = B_1\cosh\beta\bar{y} + B_2\sinh\beta\bar{y} + B_3 \tag{39}$$

$$\phi_h = -C(B_1\sinh\beta\bar{y} + B_2\cosh\beta\bar{y}) \tag{40}$$

where

$$C = D_1\beta/D_2 h, \qquad \beta = h\sqrt{A_{44}(D_1D_4 - D_2^2)/A_{22}D_1D_3}$$

For materials considered in the present paper, β is real. The coefficients B_1 and B_2 are determined by considering continuity of ϕ at $y = 0$ and the free-edge condition

$$M_{yz}(a) = 0 \tag{41}$$

Equation (41) can be satisfied if

$$\phi_{h,y}(a) = 0 \tag{42}$$

Thus

$$\phi_h = CB_2(\tanh\beta\bar{a}\,\sinh\beta\bar{y} - \cosh\beta\bar{y}) \tag{43}$$

where $a = a/h$. Combining Eqs. (27-29), (38), (39), and (43), we obtain the strain energy release rate expression

$$G_1 = (\epsilon - \epsilon_1^T)\left[E_x h(\epsilon - \epsilon_1^T) + \sum_{i=1}^{2} A_i e^{-\lambda_i(\bar{b}-\bar{a})}\right] - (\epsilon - \epsilon_2^T)\left[E^*h(\epsilon - \epsilon_2^T) + \frac{D_5 B_2}{\cosh^2\beta\bar{a}}\right] \tag{44}$$

where $\bar{b} = b/h$ and

$$D_5 = [(A_{22}B_{12} - A_{12}B_{22})\beta - (A_{22}A_{13} - A_{12}A_{23})Ch]/A_{22}h \tag{45}$$

Continuity of v^0, w^0, and ψ at $y = 0$ can be determined from rigid body displacements and rotations but is not relevant to the results presented in this paper.

If we neglect the transient portion of Eq. (45), the energy release rate reduces to the form

$$G_I = h[E_x(\epsilon - \epsilon_1^T)^2 - E^*(\epsilon - \epsilon_2^T)^2] \tag{46}$$

For cases in which thermal stresses are not included ($\Delta t = 0$), Eq. (46) reduces to the energy release rate expression derived by O'Brien[2] and illustrated in Fig. 1, i.e.,

$$G_I = h\epsilon^2(E_x - E^*) \tag{47}$$

Numerical Results

Numerical results are now considered for laminates with the following ply properties

$$E_1/E_2 = 14, \qquad G_{12}/E_2 = 0.533, \qquad G_{23}/E_2 = 0.323$$

$$E_3/E_2 = 1, \qquad \nu_{12} = 0.3, \qquad \nu_{23} = 0.55$$

$$\alpha_1 = -9\times10^{-7}/°\text{C}, \qquad \alpha_2 = \alpha_3 = 23\times10^{-6}/°\text{C} \tag{48}$$

where these properties are relative to an x_1, x_2, and x_3 axes system parallel to the fibers, transverse to the fibers, and through-the-thickness, respectively. Moduli in the x_i direction are denoted by E_i, while G_{ij} denote shear moduli relative to the x_i-x_j plane. Poisson ratios, ν_{ij}, are determined by measuring the contraction in the x_j direction during a uniaxial tensile test in the x_i direction. Thermal expansion coefficients in the x_i direction are denoted by α_i. The properties in Eq. (48) are typical of current high-performance graphite/epoxy unidirectional composites. Values of Q_{ij} and C_{ij} can be determined from the properties in Eq. (48) by using standard relationships.[10]

The stress distribution ahead of the crack, Eq. (24), is shown in Fig. 3 for a $[30/-30_2/30/90_2]_s$ laminate under tensile loading. These results do not include the effect of residual stresses. For the angle-ply laminates of the class $[\theta/-\theta_2/\theta/90_2]_s$ temperature has little effect on the shape of the stress distribution ahead of the crack but does influence the maximum stress which occurs at the crack front ($y = 0$). Such differences are illustrated in Table 1, where the average stress near the crack tip is shown for a variety of laminate orientations. Note that the stacking sequence must be reversed for compression loading, i.e., the angle-ply geometry must be of the class $[90_2/\theta/-\theta_2/\theta]_s$ in order to produce a positive σ_z at the crack tip under compression loading. In

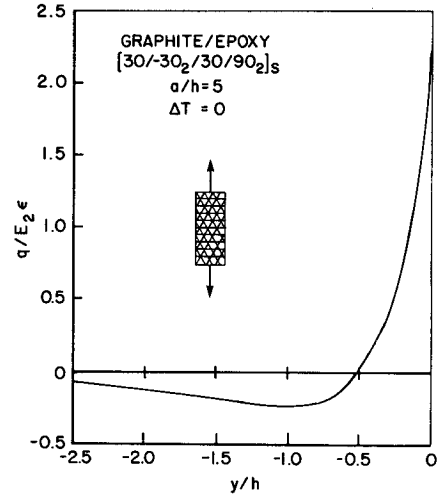

Fig. 3 Stress distribution ahead of the crack at the midplane of an angle-ply laminate.

Table 1 Average stress near crack tip (graphite/epoxy $a/h = 5$)

Orientation	ΔT (°C)	ϵ (%)	$\bar{q}/E_2\epsilon$
$[30/-30_2/30/90_2]_s$	0	+	1.894
$[30/-30_2/30/90_2]_s$	−117	+0.3	2.375
$[90_2/30/-30_2/30]_s$	0	−	1.725
$[90_2/30/-30_2/30]_s$	−117	−0.3	1.287
$[45/-45_2/45/90_2]_s$	0	+	1.495
$[45/-45_2/45/90_2]_s$	−117	+0.3	1.682
$[0_3/90_3]_s$	0	+	0.2109
$[0_3/90_3]_s$	−117	+1.0	0.4186

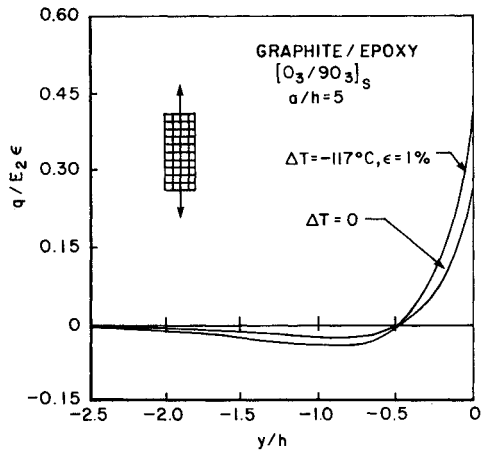

Fig. 4 Stress distribution ahead of the crack at the midplane of a bidirectional laminate.

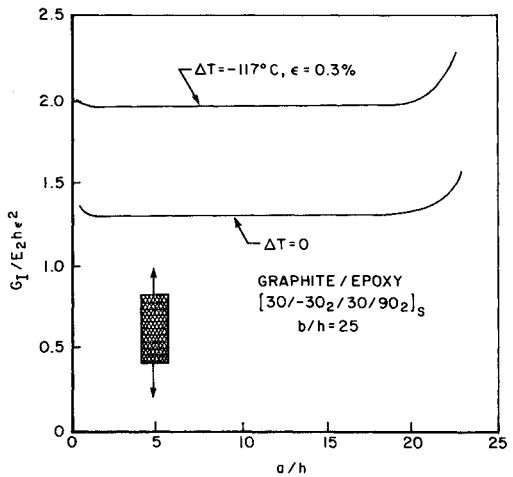

Fig. 5 Mode I strain energy release rate as a function of crack length for a 30-deg angle-ply laminate under tensile loading.

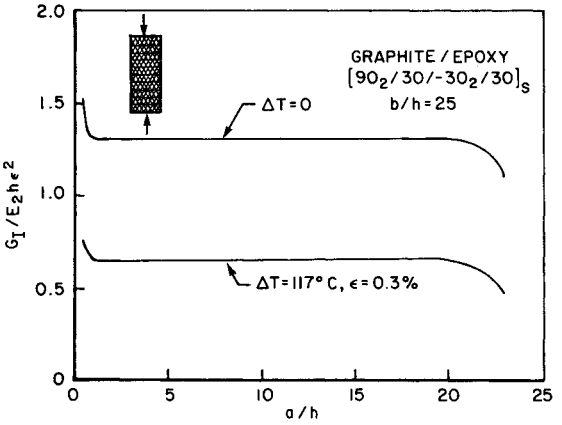

Fig. 6 Mode I strain energy release rate as a function of crack length for a 30-deg angle-ply laminate under compression loading.

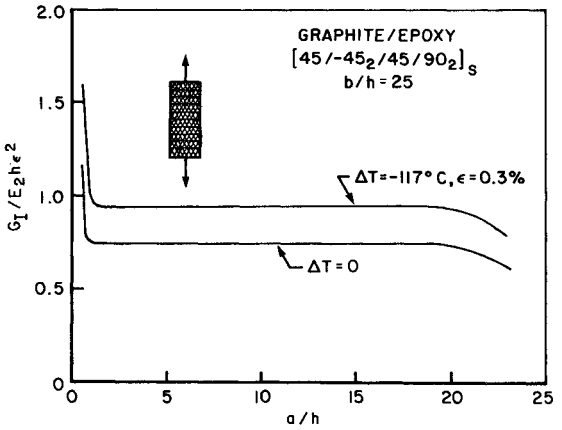

Fig. 7 Mode I strain energy release rate as a function of crack length for a 45-deg angle-ply laminate under tensile loading.

such cases residual stress produces a compression σ_z at the crack tip. Thus the stress at the crack front in the case of compressive loading is reduced by the presence of residual stresses due to composite fabrication.

For the cases where $\Delta T=0$, the axial strain ϵ can be normalized out of the solution. In the residual stress case, however, normalization requires that the ratio $\Delta T/\epsilon$ be prescribed. Thus a strain level, as well as a value of ΔT, is given in such examples. The strain level of $\epsilon=0.3\%$ for the angle-ply laminates is near ϵ_c as determined experimentally for typical angle-ply laminates.[3] In the case of the bidirectional class of laminates, $[0_3/90_3]_s$, the value of ϵ is chosen to be much larger, as ϵ_c will be much larger for such laminates. This is because in the absence of thermal residual stresses, the curvature due to bending-extensional coupling, which determines the magnitude of σ_z near the crack front, depends on the mismatch between the effective Poisson ratios ν_{xy} of the ply units in the laminate. The example, the mismatch between the ratio ν_{xy} for $[\pm\theta]_s$ laminates and that for $[90_2]$ laminates is much greater than between the ratios for $[0_3]$ laminates and $[90_3]$ laminates. In particular, the $[\pm\theta]_s$ laminates can produce values of ν_{xy} in excess of unity. For $[0_3]$ laminates, $\nu_{xy}=\nu_{12}=0.3$ is a typical value. For units of 90 deg plies, $\nu_{xy}=\nu_{21}=0.021$ is a typical value. In the case of thermal residual stresses, the mismatch between the effective thermal expansion coefficients α_y of the ply units determines the intensity of σ_z at the crack front. Angle-ply units of the class $[\pm\theta]_s$ have much lower values of α_y than do $[0_3]$ units. In addition, for $[90_n]$ laminates, $\alpha_y=\alpha_2=-0.9\times10^{-6}/°C$ for the material under consideration. Thus both the $[\theta/-\theta_2/\theta/90_2]_s$ and $[0_3/90_3]_s$ classes of laminates can produce considerable mismatch between ply units, but the bidirectional class is much more significant. This is also illustrated in Table 1 and in Fig. 4, where the shape of the stress distribution ahead of the crack is drastically changed owing to thermal effects, as well as the average stress $\bar{q}$ near the crack tip, which is defined as

$$\bar{q}=\frac{1}{h_0}\int_{-h_0}^{0} q\,dy \tag{49}$$

where h_0 is taken as one ply thickness, i.e., $h_0=h/12$. An average stress is utilized because of the presence of a crack tip singularity in an exact elasticity solution which renders the magnitude of q at the crack tip meaningless in an approximate analysis.

Normalized values of mode I strain energy release rate are shown in Figs. 5-8. A cursory examination of Eq. (44) and the results in Figs. 5-8 reveal that two parameters govern the value of G_I for a given laminate: a/h and b/h. For current EDT specimens $b/h=25$ is typical. This assumes $2b=38$ mm (1.5 in.), while for a 12-ply graphite/epoxy laminate $2h=1.52$ mm (0.06 in.). For the laminates loaded in tension, residual stresses increase the energy release rate. This is due to the asymmetric nature of the upper half of the laminates under consideration, i.e., laminates of the class $[\theta/-\theta_2/\theta/90_2]_T$ and $[0_3/90_3]_T$ will open outward under

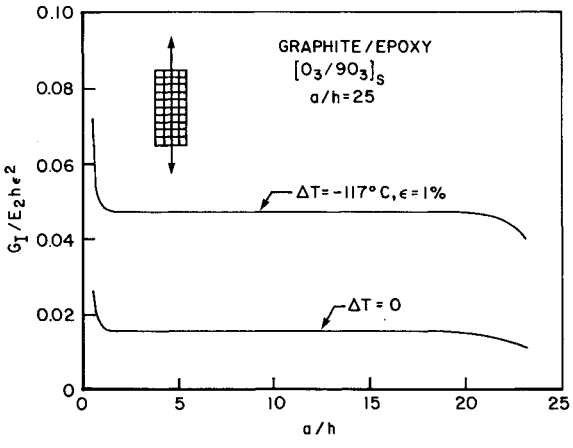

Fig. 8 Mode I strain energy release rate as a function of crack length for a bidirectional laminate under tensile loading.

negative values of ΔT, resulting in an initial stress at the crack front which must be accounted for in the determination of critical strain energy release rates G_{Ic}. For the $[0_3/90_3]_T$ class of asymmetric laminate, the initial curvature due to residual stress is very large. Thus in this case, as illustrated in Fig. 8, the effect of residual stress on G_I is very large. For the case of compression loading (see Fig. 6) and the $[90_2/\theta/-\theta_2/\theta]$ class of laminates, residual stresses tend to close the crack owing to reversal of stacking sequence. As a result, residual stresses reduce values of G_I. From Figs. 5-8 it can easily be seen that G_I is independent of crack length for a wide range of practical values of a/h.

The cure temperature for standard graphite/epoxy laminates is 177°C (350°F). If we consider room temperature to be 21°C (70°F), then the maximum value of ΔT for room temperature consideration is −156°C. Data obtained by Pagano and Hahn[11] on the load-free deformation of asymmetric laminates indicates a stress-free temperature in the range of 121°C (250°F) to 149°C (300°F). The value of $\Delta T = -117$°C is obtained by assuming a stress-free temperature of 138°C (280°F). Although the dramatic increase in G_I with decreasingly small values of a/h, as observed in Figs. 5-8, suggests that G_I becomes unbounded as the crack length vanishes, an examination of Eq. (44) reveals that G_I does not become singular as $a/h \to 0$. Such small values of a/h are of little practical interest, and the precise behavior of G_I in this range is only of academic interest.

Conclusions

A higher-order laminated plate theory has been utilized to obtain an approximate solution to the normal stress distribution ahead of the crack in a mode I edge delamination specimen containing a starter crack. The analysis is also used to assess the effect of specimen geometry and thermal residual stresses due to laminate fabrication on the mode I strain energy release rate. In the analysis the plate is divided into a section along the crack and a second section along the uncracked region. Complete continuity of force resultants, bending moment, and displacments are satisfied across the boundary between the two sections.

Numerical results are presented fo 12-ply laminates of the classes $[\theta/-\theta_2/\theta/90_2]_s$, $[0_3/90_3]_s$, and $[90_2/\theta/-\theta_2/\theta]_s$. Tensile loading is considered in conjunction with the first two laminates, and compression loading in conjunction with the third laminate. The following conclusions are drawn from the numerical results:

1) The effect of the normal stress ahead of the crack dissipates within a distance of approximately $2h$ from the crack front.

2) The mode I energy release rate G_I is independent of crack length over the interval $0.5h \le a \le b - 5h$.

3) Residual stresses due to fabrication increase the magnitude of the stress at the crack tip for tensile EDT specimens, and reduce the magnitude for compression EDT specimens.

4) Residual stresses due to fabrication increase G_I for tensile EDT specimens and reduce G_I for compression EDT specimens.

5) Residual stresses due to fabrication can have a significant influence on both the stress distribution at the crack front and G_I.

The conclusion concerning residual stress effects needs additional consideration. In particular, residual stresses due to composite fabrication can be reduced in epoxy resin materials by the presence of moisture. In most applications, however, the distribution of moisture through the thickness will not be uniform. Thus the combined effects of moisture and temperature may produce complex results on both the stress distribution ahead of the crack and the mode I strain energy release rate. In structural problems such as delamination and buckling, residual stresses may be significant. To date, residual stresses have not been considered in such problems.

References

[1]Pagano, N. J. and Pipes, R. B., "Some Observations on the Interlaminar Strength of Composite Laminates," *International Journal of Mechanical Sciences*, Vol. 15, 1973, pp. 679-688.

[2]O'Brien, T. K., "Characterization of Delamination Onset and Growth in a Composite Laminate," *Damage in Composite Materials*, ASTM STP 775, K. L. Reifsnider (ed.), American Society for Testing and Materials, Philadelphia, 1982, pp. 140-167.

[3]Whitney, J. M. and Knight, M., "A Modified Free-Edge Delamination Specimen," *Delamination and Debonding of Materials*, ASTM STP 876, edited by W. S. Johnson, Philadelphia, 1985, pp. 298-314.

[4]Pagano, N. J., "On the Calculation of Interlaminar Normal Stress in Composite Laminates," *Journal of Composite Materials*, Vol. 8, Jan. 1974, pp. 65-82.

[5]Whitney, J. M., "Stress Analysis of the Double Cantilever Beam Specimen," *Composite Science and Technology*, Vol. 23, No. 2, 1985, pp. 201-219.

[6]Whitney, J. M. and Pagano, N. J., "Shear Deformation in Heterogeneous Anisotropic Plates," *Journal of Applied Mechanics*, Vol. 37, Dec. 1970, pp. 1031-1036.

[7]Whitney, J. M. and Sun, C. T., "A Higher Order Theory for Extensional Motion of Laminated Composites," *Journal of Sound and Vibration*, Vol. 30, No. 1, 1978, pp. 85-97.

[8]Medwadowski, S. J., "A Refined Theory for Elastic Orthotropic Plates," *Journal of Applied Mechanics*, Vol. 25, March 1958, pp. 437-443.

[9]Pagano, N. J., "Exact Moduli of Anisotropic Laminates," *Composite Materials, Mechanics of Composite Materials*, Vol. 2, edited by G. P. Sendeckyj; L. J. Broutman and R. H. Krock series editors, Academic, New York, pp. 23-44.

[10]Jones, R. M., *Mechanics of Composite Materials*, McGraw-Hill, New York, 1975.

[11]Pagano, N. J. and Hahn, H. T., "Evaluation of Composite Curing Stresses," *Composite Materials: Testing and Design (Fourth Conference)*, ASTM STP 617, American Society for Testing and Materials, Philadelphia, 1977, pp. 371-329.